

**The CERN-EU high-energy Reference Field (CERF) facility  
for dosimetry at commercial flight altitudes and in space**

Angela Mitaroff and Marco Silari

**ABSTRACT**

A reference facility for the calibration and inter-comparison of active and passive detectors in broad neutron fields has been available at CERN since 1992. A positively charged hadron beam (a mixture of protons and pions) with momentum of usually 120 GeV/c hits a copper target, 50 cm thick and 7 cm in diameter. The secondary particles produced in the interaction traverse a shield, at 90° with respect to the direction of the incoming beam, made of either 80 to 160 cm of concrete or 40 cm of iron. Behind the iron shield, the resulting neutron spectrum has a maximum at about 1 MeV, with an additional high-energy component. Behind the 80 cm concrete shield, the neutron spectrum has a second pronounced maximum at about 70 MeV and resembles the high-energy component of the radiation field created by cosmic rays at commercial flight altitudes. This paper describes the facility, reports on the latest neutron spectral measurements, gives an overview of the most important experiments performed by the various collaborating institutions over the past years, addresses the possible application of the facility to measurements related to the space programme and discusses the latest calculations performed in view of its development for such use.

*Submitted for publication in Radiation Protection Dosimetry*

CERN, 1211 Geneva 23, Switzerland  
28 March 2001

## INTRODUCTION

In its 1990 recommendations the International Commission on Radiological Protection (ICRP) stated that exposure of civil aircrew has to be considered as being occupational <sup>(1)</sup>. This has been translated into a legal requirement in the European Union in 1996 by the Council Directive 96/29 <sup>(2)</sup>. The ICRP recommendations have boosted several research activities worldwide aiming at determining dose equivalent rates for the various commercial routes as well as establishing experimental and computational tools for dosimetry of aircrews. In this framework the European Union has sponsored since 1992 co-ordinated actions with the aim to merge the expertise of several research institutions in the field of cosmic ray physics and dosimetry <sup>(3-6)</sup>. A wide range of active instruments and passive devices has been employed in several measurement campaigns, mainly on-board commercial flights but also on some dedicated flights (see, for example, refs. <sup>(3,4,7-13)</sup>).

If both the energy and angle response characteristics of a device and the energy and direction distribution of the radiation field to be determined are well known, the response data can be folded with the field data to obtain a response correction factor. In practice these conditions are rarely met for in-flight measurements. An alternative approach is thus to determine the response of the device either in the radiation field of interest (a “field calibration”) or in a experimental radiation field of sufficiently similar characteristics (a “simulated workplace field”) (Figure 1).

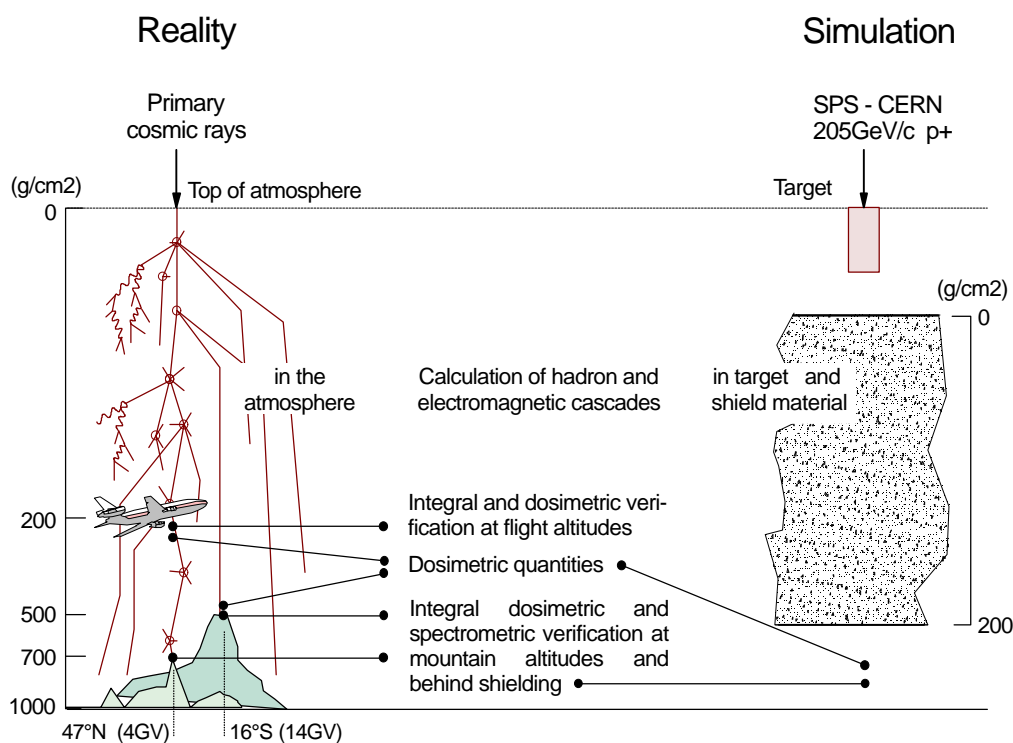


**Fig. 1.** The cosmic radiation field in the atmosphere and its simulation at CERN.

The direct field calibration in aircraft requires a reference instrument in principle capable of determining the true value of ambient dose equivalent for all radiation components and energies. In this respect the tissue equivalent proportional counter (TEPC) is presently considered the best suited instrument for field calibration in the cosmic radiation field at flight altitudes<sup>(14)</sup>. However, the availability of a reference radiation facility providing particle composition and spectral fluences similar to those in the cosmic radiation field at commercial flight altitudes (10-20 km) is of obvious interest. The EU funded programmes placed significant emphasis on calibration and characterisation of detectors. An important element in these programmes is the simulation of the cosmic ray field at aircraft altitudes at an experimental facility available at CERN, which provides a reference base for both passive and active instruments<sup>(15)</sup>.

The facility is a development of an idea conceived by Stevenson in 1987, when an experimental area was set-up to study the spatial distribution of hadron and low-energy neutron fluence and of absorbed dose in the cascades induced in iron and lead calorimeter structures irradiated by high-energy hadron beams. These experiments (the so-called Röstli series of experiments)<sup>(16-18)</sup> were organised to investigate possible neutron damage to detector systems for the new generation of hadron colliders, namely the Large Hadron Collider (LHC) planned at CERN and the Super-conducting Super-Collider (SSC) at that time under construction in the USA. The experiments were also intended to provide benchmarks for Monte Carlo codes simulating the development of hadron-induced cascades<sup>(19)</sup>. At that time the experimental area simply consisted of a thick iron or lead block surrounded by a concrete shield. The CERN reference radiation facility is a development of these experiments; it was set-up in 1992 and subsequently upgraded to its present form in 1993. In addition to the interest for testing active instrumentation and passive detectors used around high-energy particle accelerators, this reference field is sufficiently similar to the cosmic ray field encountered at 10-20 km altitude such that instrumentation is tested, inter-compared and calibrated at CERN and subsequently used for in-flight measurements on aircraft.

The aim of the present paper is to describe the facility, which has previously been illustrated only in two conference proceedings<sup>(20,21)</sup>, report on the latest neutron spectral measurements, give an overview of the most important experimental investigations carried out by the various collaborating institutions over the past years, address its possible application to measurements related to the space programme and discuss the latest calculations performed in view of its upgrade for such use.

## **THE CERN-EU HIGH-ENERGY REFERENCE FIELD (CERF) FACILITY**

The CERN-EU high-energy Reference Field (CERF) facility is installed in one of the secondary beam lines (H6) from the Super Proton Synchrotron (SPS), in the North Experimental Area on the Prévessin (French) site of CERN (Figures 2 and 3). (Incidentally, *cerf* in French means *deer*: there is a fenced area where several deer live close to the experimental hall where CERF is operational.) A positive hadron beam with momentum of usually 120 GeV/c is stopped in a copper target, 7 cm in diameter and 50 cm in length, which can be installed in two different positions inside an irradiation cave. In the past 205 GeV/c positive and negative hadron beams (respectively a mixture of about 2/3 protons and 1/3 positive pions or negative pions) were also used. The secondary particles produced in the target traverse a shielding, on top of these two positions and at 90° with respect to the incoming beam direction, made up of either 80 cm concrete or 40 cm iron. These roof-shields produce almost uniform radiation fields over two areas of 2x2 m<sup>2</sup>, each of them divided into 16 squares of 50x50 cm<sup>2</sup>. Each element of these “grids” represents a reference exposure location.

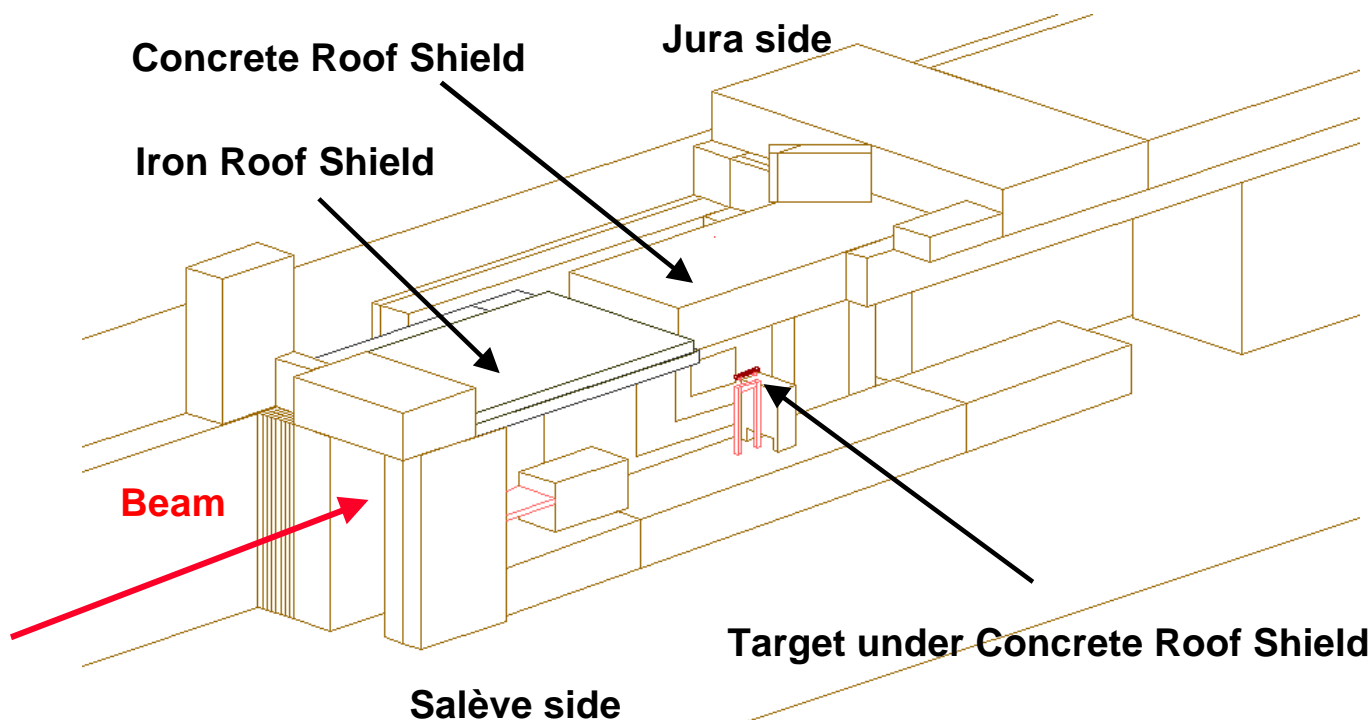


**Fig. 2.** Axonometric view of the CERF facility in the North Experimental Hall on the Prévessin site of CERN as modelled in FLUKA. The side shielding on the Salève side is removed to show the inside of the irradiation cave with the copper target set-up.

Additional measurement positions are available behind the lateral shielding of the irradiation cave, at the same angles with respect to the target as for the two roof positions. Shielding is either 80 cm or 160 cm concrete, and at both positions 8 additional exposure locations (arranged in 2x4 grids made up of the same 50x50 cm<sup>2</sup> elements) are provided. The nominal measurement locations (the reference field) are at the centre of each square at 25 cm above floor, i.e. at the centre of a 50x50x50 cm<sup>3</sup> air volume, where the radiation field is calculated. The intensity of the primary beam is monitored by an air-filled Precision Ionisation Chamber (PIC) at atmospheric pressure, placed in the beam just upstream of the copper target, connected to a current digitising circuit. One PIC-count corresponds (within  $\pm 10\%$ ) to  $2.2 \times 10^4$  particles impinging on the target. Typical values of dose equivalent rates are 1-2 nSv per PIC-count on top of the 40 cm iron roof-shield and 0.3 nSv per PIC-count outside the 80 cm concrete shields (roof and side). By adjusting the beam intensity on the target one can vary the dose equivalent rate at the reference positions, typically in the range from 25  $\mu\text{Sv/h}$  to 1 mSv/h on the iron roof-shield and from 5 to 600  $\mu\text{Sv/h}$  on the 80 cm concrete roof or lateral shield. The dose equivalent rate outside the 160 cm thick concrete shield is much lower and for this reason this measurement position is seldom used. The energy distributions of the various particles (mainly neutrons, but also photons, electrons, muons, pions and protons) at the various exposure locations have been obtained by Monte Carlo simulations performed with the FLUKA code<sup>(22,23)</sup>. Details of the latest simulations are given in ref.<sup>(21)</sup>. Here we shall just recall that the entire experimental area was accurately modelled using combinatorial geometry. Calculations were performed for four cases, i.e. beam momentum of 120 GeV/c or 205 GeV/c and positive or negative particles. The  $\pm 205$  GeV/c and the negative 120 GeV/c beams were used in the past, whilst since 1996 all experiments are performed with a beam of +120 GeV/c particles. The neutron and photon energy distributions calculated for a primary beam of positive particles with 120 GeV/c momentum (35% protons, 61% pions and 4% kaons, as determined experimentally) are shown in Figure 4.

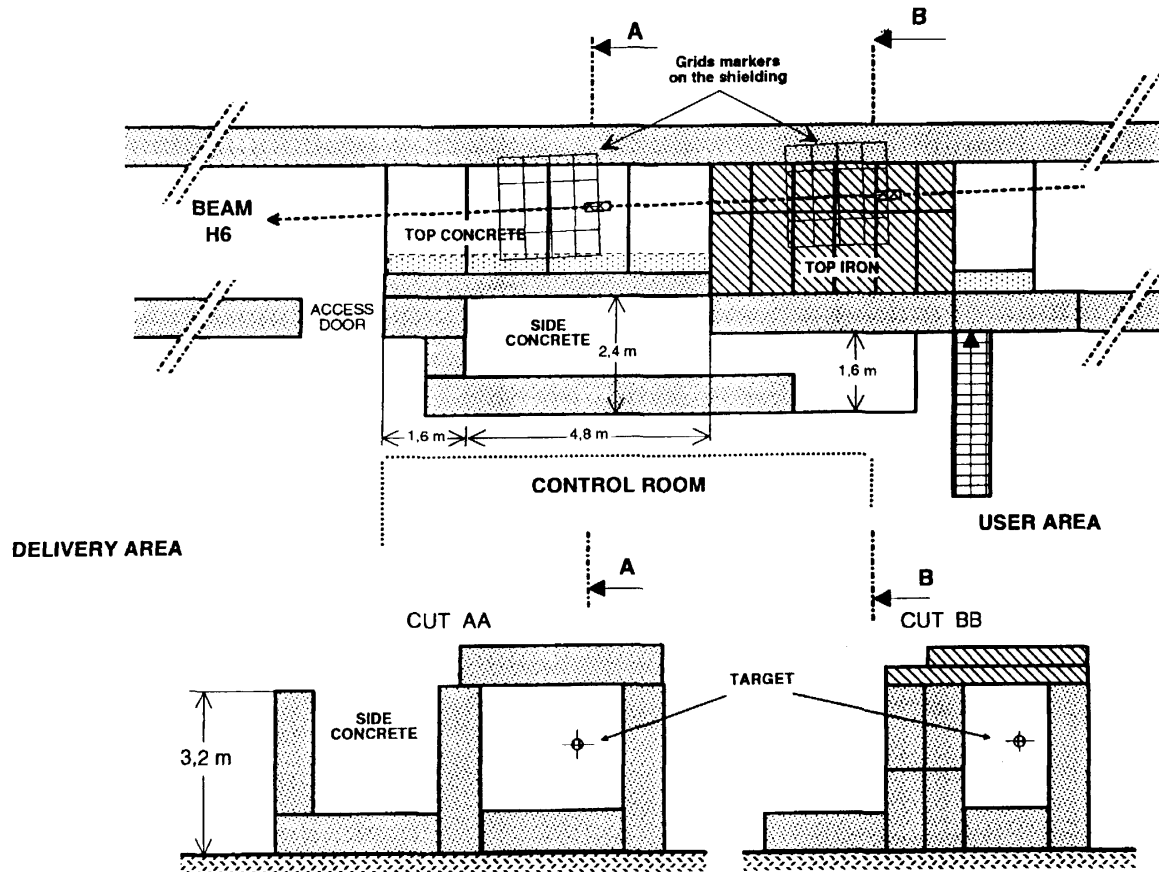


Fig. 3a. Plan and sectional views of the CERF facility.

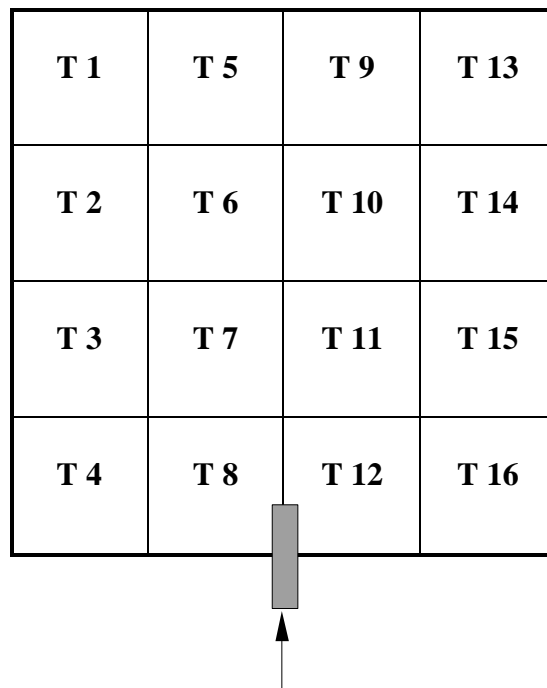
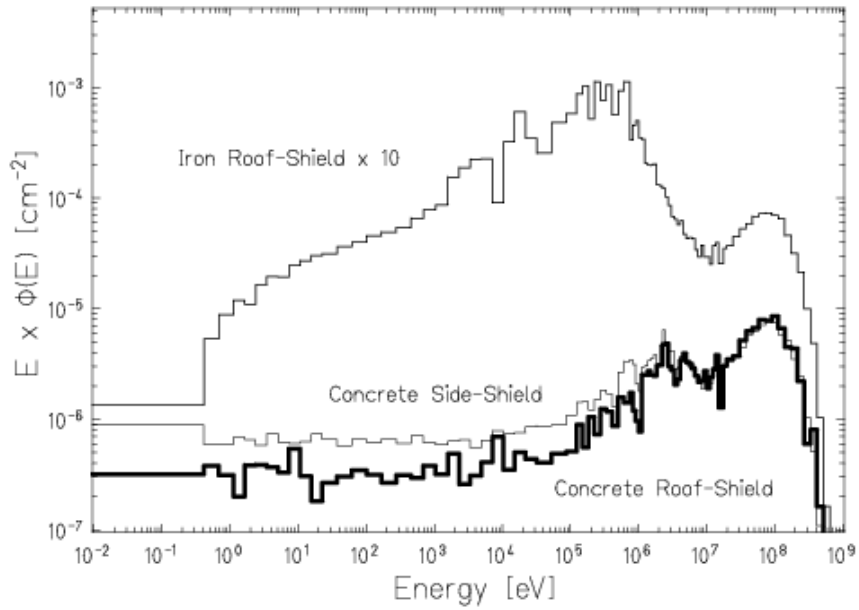
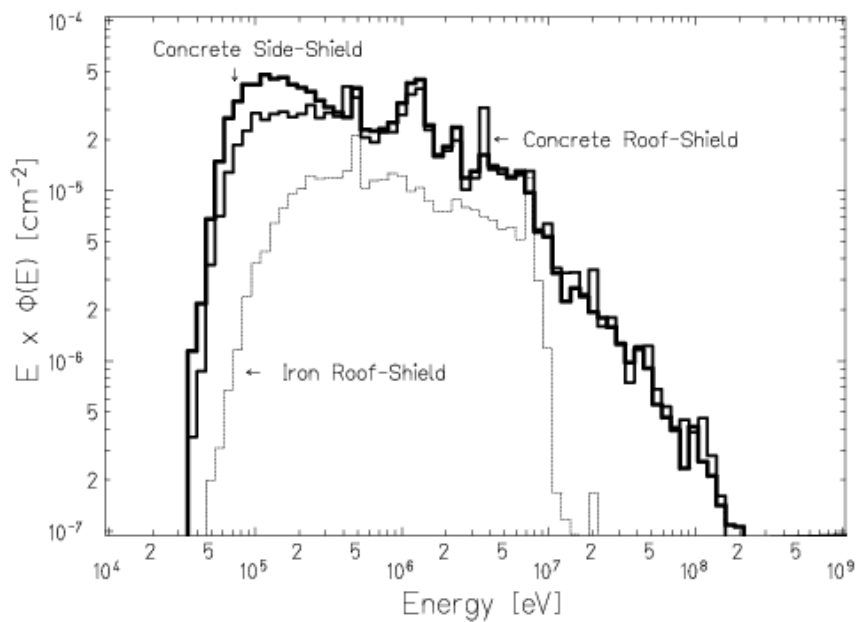


Fig. 3b. The reference grid with the 16 exposure locations used on the concrete and iron roof shields.



**Fig. 4a.** Neutron spectral fluences (lethargy) on the concrete roof-shield, on the iron roof-shield and on the 80 cm thick concrete side-shield (neutrons per primary beam particle incident on the copper target).



**Fig. 4b.** Photon spectral fluences (lethargy) on the concrete roof-shield, on the iron roof-shield and on the 80 cm thick concrete side-shield (neutrons per primary beam particle incident on the copper target).

In general the neutron energy distributions do not change in shape from 120 GeV/c to 205 GeV/c, for either positive or negative particles, and only the absolute fluence is larger for the higher energy. The spectrum outside the iron shield is dominated by neutrons in the 0.1 – 1 MeV range. The energy distribution outside the concrete shield shows an additional large relative contribution of 10 – 100 MeV neutrons. Therefore these exposure locations provide wide spectrum radiation fields well suited to test dosimetric instrumentation under different conditions. The latter, in particular, reproduces fairly closely the neutron field produced by cosmic rays at commercial flight altitudes <sup>(14)</sup>. The neutron spectral fluence behind the side 80 cm thick concrete shield is similar, but presents an increased low energy tail due to backscatter. The fluence rate of other hadrons is much lower than that of neutrons. As seen from Figure 4, the photon fluence is almost one order of magnitude less than that of neutrons on the iron roof-shield, but almost a factor two higher than the neutron fluence on the concrete roof-shield, because of the contribution from (n,γ) reactions. The electron fluence is about one order of magnitude less than that of neutrons and the muon fluence almost three orders of magnitude less. However, an additional muon component is also present which directly comes from the upstream H6 beam line and adjacent lines, as well as from pion decay in the beam line. These muons stream over the concrete and iron roof-shields. Their intensity depends on various factors which are not under direct control, such as the intensity of secondary beams in neighbouring beam lines. This contribution is discussed in some more detail below.

The accuracy of the calculated neutron spectral fluences was verified in the past by extensive measurements made first with a BF<sub>3</sub> proportional counter enclosed in polyethylene cylinders of different thickness <sup>(24)</sup> and subsequently with a Bonner sphere spectrometer (BSS). Past measurements were done with a standard BSS <sup>(21)</sup>: a <sup>3</sup>He proportional counter employed bare and within a set of five polyethylene spheres (83 mm, 108 mm, 133 mm, 178 mm and 233 mm in diameter), with the addition of the spherical version of the LINUS rem counter as high-energy channel <sup>(25-28)</sup>. The excellent agreement found between the FLUKA predictions and the experimental results was confirmed by recent neutron spectrometry measurements performed with a BSS which now includes two dedicated high-energy channels based on the LINUS design <sup>(29,30)</sup>.

Of these two new channels, the first (“olloio”) is a sphere with a diameter of 255 mm and consists of (from the central <sup>3</sup>He proportional counter outwards) 3 cm polyethylene, 1 mm cadmium, 1 cm lead and 7 cm polyethylene thickness. This configuration suppresses the response to incident neutrons with energies lower than 100 keV and increases it for energies above 10 MeV and up to 1 GeV, as compared to the 233 mm sphere of our conventional BSS. However the response function still shows the peak at about 10 MeV. The second detector (“stanlio”), with a diameter of 118.5 mm, consists of 2 cm polyethylene, 1 mm cadmium and 2 cm lead thickness and does not show the peak at 10 MeV. At low energies it behaves like a small Bonner Sphere, but at high energies the response is increased compared to the 233 mm sphere. The measurements were performed with a +120 GeV/c hadron beam on the concrete roof-shield of CERF, exactly in the same position where the spectrum had been calculated with FLUKA, i.e. 25 cm above the concrete roof shielding on top of the copper target. The beam intensity was tuned sufficiently low to prevent dead time and pile-up effects. Before each measurement the beam was switched off to determine the background coming from other beam lines and experiments in the hall. The computed response functions of the extended BSS to monoenergetic neutrons were folded with the spectral fluences of ref. <sup>(21)</sup> and compared with the experimental count rates. These latest results are given in Table 1. The quoted uncertainties are only statistical but take the correlation of the computed response functions and the fluence spectra into account when summing-up over the energy bins. However, they do not include systematic uncertainties in the detector efficiency and in the FLUKA code.

**Table 1.** Experimental and calculated absolute response of the extended Bonner Sphere Spectrometer to the broad neutron spectrum on the concrete roof-shield of CERF, for a 120 GeV/c positive hadron beam (61% pions, 35% protons and 4% kaons) impinging on the copper target.

Sphere	Response (counts per incident hadron on the copper target)		
	Experimental	Calculated	Ratio (calc/exp)
83 mm + cadmium	$(1.38\pm 0.07)\times 10^{-5}$	$(1.56\pm 0.26)\times 10^{-5}$	1.13 $\pm$ 0.19
83 mm	$(2.01\pm 0.09)\times 10^{-5}$	$(2.30\pm 0.31)\times 10^{-5}$	1.14 $\pm$ 0.16
108 mm	$(2.72\pm 0.12)\times 10^{-5}$	$(2.87\pm 0.42)\times 10^{-5}$	1.06 $\pm$ 0.16
133 mm	$(3.19\pm 0.15)\times 10^{-5}$	$(3.20\pm 0.47)\times 10^{-5}$	1.00 $\pm$ 0.15
178 mm	$(3.23\pm 0.15)\times 10^{-5}$	$(3.30\pm 0.47)\times 10^{-5}$	1.02 $\pm$ 0.15
233 mm	$(2.81\pm 0.13)\times 10^{-5}$	$(2.96\pm 0.40)\times 10^{-5}$	1.05 $\pm$ 0.15
Stanlio	$(1.58\pm 0.07)\times 10^{-5}$	$(1.93\pm 0.29)\times 10^{-5}$	1.22 $\pm$ 0.20
Ollio	$(1.93\pm 0.09)\times 10^{-5}$	$(2.36\pm 0.32)\times 10^{-5}$	1.22 $\pm$ 0.17

The reference values of neutron ambient dose equivalent,  $H^*(10)$ , on the concrete and iron roof-shields are given in Table 2 for a 120 GeV/c positive beam. The values are obtained by folding the neutron spectral fluence calculated by FLUKA at the centre of each of the 16 squares of the grid, 25 cm above the shield (i.e., at the centre of a  $50\times 50\times 50$  cm<sup>3</sup> air volume) with the fluence-to-ambient dose equivalent conversions coefficients of ICRP74 (up to 19 MeV) <sup>(31)</sup> and of Ferrari and Pelliccioni (above 19 MeV) <sup>(32)</sup>. The values are mapped according to the grid shown in Figure 3(b). The statistical uncertainties of the Monte Carlo calculations are less than 2% for the concrete shield and less than 1% for the iron shield. The values are normalised to one unit of the beam monitor (PIC-count).

**Table 2.** Reference values of neutron ambient dose equivalent,  $H^*(10)$ , on the concrete and iron roof-shields, for a beam of positive particles with 120 GeV/c momentum (35% protons, 61% pions and 4% kaons) incident on the copper target. The values are mapped according to the grid shown in Figure 3(b). The statistical uncertainties are less than 2% for the calculations for the concrete shield and less than 1% for the iron shield. The  $H^*(10)$  values are normalised to one unit of the beam monitor (PIC-count), with one PIC-count =  $2.2\times 10^4$  hadrons impinging on the target.

Neutron ambient dose equivalent, $H^*(10)$ (pSv per PIC-count)							
Concrete roof-shield				Iron roof-shield			
216	254	253	207	1041	1286	1203	732
225	270	270	222	1170	1490	1454	1002
213	267	265	207	1238	1602	1596	1099
185	223	221	182	1137	1493	1471	1005

The microdosimetric spectra measured on the concrete and iron roof-shields as well as on the 80 cm thick concrete side-shield by the HANDI TEPC are shown in Figure 5. The similarity of the absorbed dose spectra on the concrete roof-shield and at flight altitude <sup>(33)</sup> is shown in Figure 6.



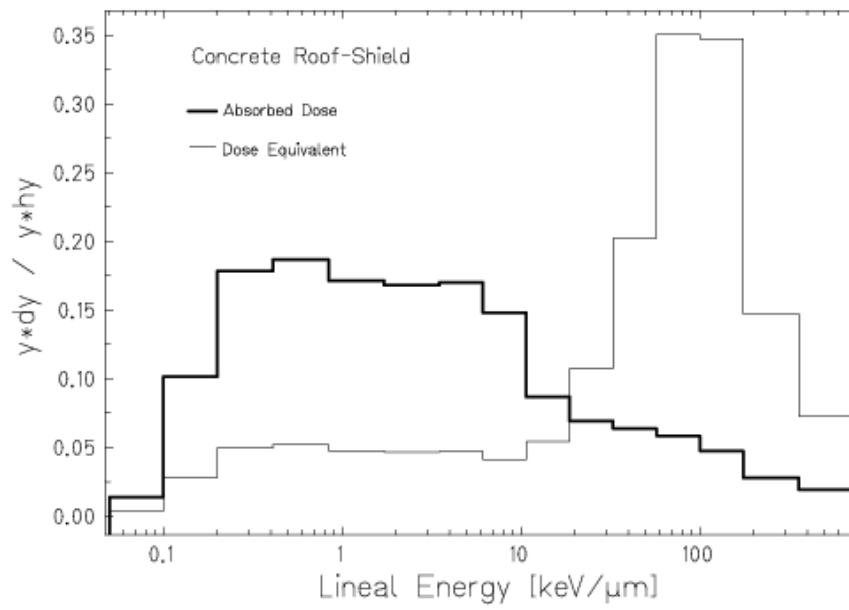


**Fig. 5a.** Microdosimetric spectra measured on the concrete roof-shield with the HANDI TEPC.

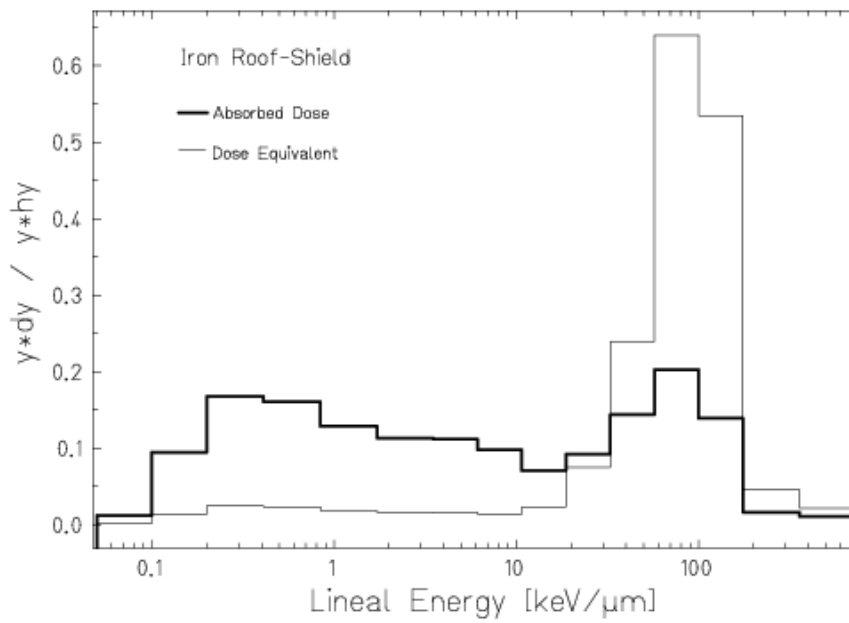


**Fig. 5b.** Microdosimetric spectra measured on the iron roof-shield with the HANDI TEPC.

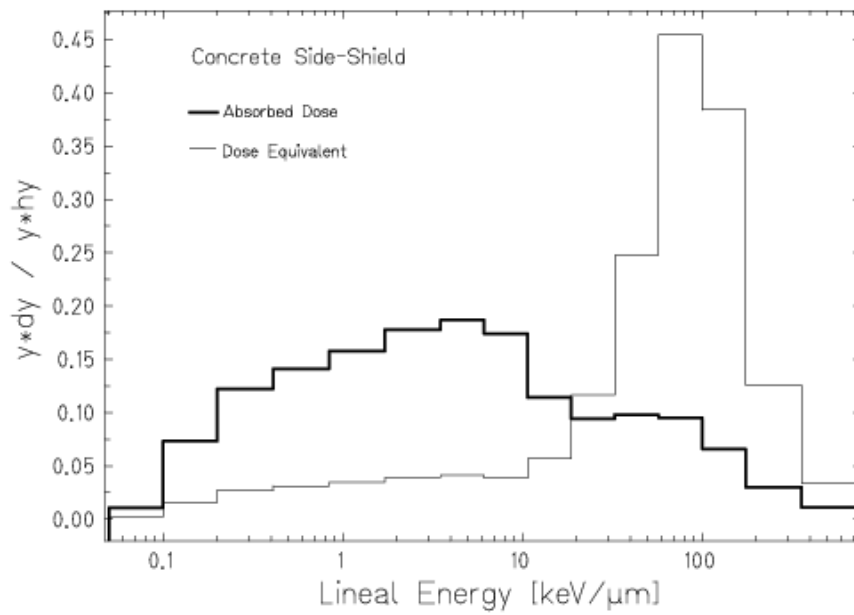


**Fig. 5c.** Microdosimetric spectra measured on the 80 cm thick concrete side-shield with the HANDI TEPC.

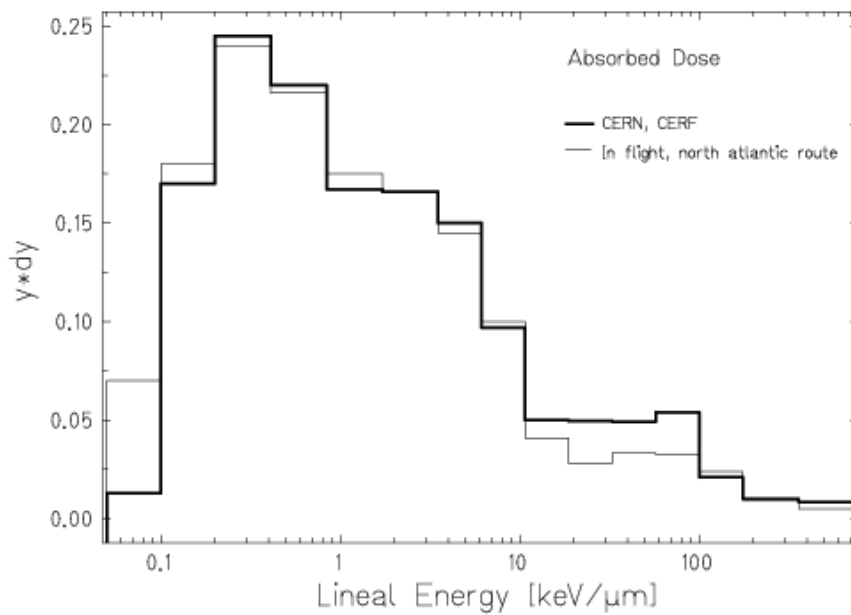


**Fig. 6.** Absorbed dose spectra on the concrete roof-shield of CERF and at flight altitude on a north Atlantic route <sup>(33)</sup>.

## MUON BACKGROUND

At the measurement sites on the concrete and iron roof-shields there is a significant low-LET background radiation field. This background, which is timed to the pulsed structure of the beam, is not coming from interaction of the beam in the copper target but is mainly due to high-energy muons originating from pion decay in the beam line, with some contribution from hadron beam losses upstream in the H6 or neighbouring beam lines. If not taken into account, this background appears as an apparent non-linearity of a detector response when measurements are performed at different intensities of the incident hadron beam. This concerns ionisation chambers, TEPC and other active devices that have considerable sensitivity to low-LET radiation. On the other hand, there is no significant muon background at the side concrete shielded positions.

Various methods of muon background subtraction from TEPC measurement data were investigated during the May 1994 run with a 205 GeV/c beam<sup>(34)</sup>. The distribution of muons on the roof-shields was studied during the May 1995 run<sup>(35)</sup>, again with a 205 GeV/c beam, with the help of a counter telescope using the fact that these high energy muons are strongly directional and travel parallel to the primary beams. This experiment allowed a number of conclusions to be drawn. First, the muons are also present with the H6 beam switched off. This means that the muon intensity is essentially independent of the intensity of the hadron beam on the copper target and thus cannot be normalised to the PIC-counts. Second, there is a strong gradient of the muon fluence when moving from the Salève to the Jura side of the facility (Figure 2), due to a large muon contribution from the neighbouring H8 beam line on the Salève side. Third, there is a small contribution of muons coming from the H6 beam line. This additional component is however not originating from the H6 production target which is seen under a big angle, but rather from the upstream collimators that are used to limit the beam intensity and hence are a source of penetrating muons. The measured fluence rates were converted to dose using a conversion coefficient of 40 fGy m<sup>2</sup><sup>(36)</sup>. For typical high intensity beam conditions, the measured muon background was found to be between 3 and 12 pGy per PIC-count moving from the Salève side to the Jura side of the concrete roof-shield. This should be compared with total dose equivalent on the concrete roof-shield of typically 300 to 400 pSv/PIC-count respectively, of which 50 to 75 pSv/PIC-count resulting from low-LET particles (< 6 keV  $\mu\text{m}^{-1}$ ).

In the August 1996 run<sup>(37)</sup> measurements with a TEPC were performed in order to show the importance of the muon background at low beam intensities. This was demonstrated by measuring the low-LET (<6 keV/ $\mu\text{m}$ ) fraction of the dose on the iron roof-shield as a function of beam intensity, and taking into account that there is a constant component due to muons. The ratio of low-LET to total dose equivalent was found to increase from a few percent for beam intensities above about 2000 PIC-counts per SPS pulse, to about 10% at 1000 PIC-counts per pulse and up to well above 50% for low beam intensity of a few hundreds PIC-counts per pulse.

An investigation of the low-LET background radiation was later carried out with a recombination chamber<sup>(38)</sup>. Measurements of absorbed dose and the recombination index of radiation quality at different intensities of the hadron beam have shown that the value of absorbed dose per PIC-count exhibits a non-linear dependence on beam intensity on the roof-shield, while the same quantity is constant for the side location. When the same data are plotted relative to the absorbed dose per pulse, the dependence on PIC-count becomes linear and the background radiation can be determined as a component independent of the beam intensity.

Since the muon background is mostly independent of the intensity in the H6 beam line but changes with factors like beam composition (the pion fraction is a function of beam momentum) and intensity in the neighbouring beam lines, it is not exactly reproducible from run to run. Therefore the present results can only be regarded as a guideline; the background

must be checked before each experiment with low-LET sensitive devices. Nevertheless, the CERF mixed neutron, photon and muon field was used to test, before its use on-board aircraft, a method of separating TEPC pulse heights for non-charged and charged particles using an active shielding detector developed by PTB for in-flight measurements <sup>(8)</sup>.

## BEAM MONITORING

The intensity of the SPS secondary beam to CERF is monitored by a Precision Ionisation Chamber (PIC) installed just upstream of the copper target. Both the calculated spectral fluences and the data of the experiments performed at CERF are usually normalised to the intensity of the beam impinging on the target. Therefore a good knowledge of the calibration factor of the PIC is essential.

In 1993/94 a series of in-beam activation measurements were made, to characterise the beam intensity and composition (the pion to proton ratio) of different beam momenta <sup>(39-43)</sup>. For this purpose three types of carbon activation detectors were used: small plastic scintillators, graphite discs and polyethylene foils of different thickness in order to study the effect of cascade build-up as well. The reactions used were  $^{12}\text{C}(\text{p},\text{pn})^{11}\text{C}$  for protons and  $^{12}\text{C}(\pi,\pi\text{n})^{11}\text{C}$  for pions. During a run in May 1993 additional measurements with aluminium plates were performed looking at the  $^{18}\text{F}$  and  $^{24}\text{Na}$  activation. The induced activity of these detectors was measured with a 3"x3" NaI detector system by counting the 0.511 MeV gamma-rays from positron annihilation. In addition the plastic scintillator was placed after exposure in the beam on top of a 5" photomultiplier tube. The scintillator then detects its own positrons from the  $^{11}\text{C}$  decay. All these measurements gave a calibration factor of  $2.2 \times 10^4$  particles per PIC-count, with an uncertainty of  $\pm 10\%$ .

In 1998 a verification of the PIC calibration factor was carried out by comparing the response of the PIC with that of scintillators that are part of the beam line instrumentation <sup>(44)</sup>. The result of these measurements, i.e.  $22100 \pm 300$  particles per PIC-count, showed that the calibration factor was still in agreement with the 1993/94 measurements. In 1999 this method was again used to determine the calibration factor of the PIC but in a more precise way, i.e. by measuring the background and subtracting it from the detector signal, correcting the scintillator signal according to its dead time and doing a complete error analysis <sup>(45)</sup>. Two independent measurements with different data processing and analysis methods were performed, the first in May with a beam of 120 GeV/c positive hadrons, the second in August with beams of 120 GeV/c and 40 GeV/c positive hadrons. The results of these experiments gave a calibration factor of  $23250 \pm 950$  particles per PIC-count for 120 GeV/c positive hadrons and  $24500 \pm 650$  particles per PIC-count for 40 GeV/c positive hadrons, in good agreement with the previous results.

## OVERVIEW OF EXPERIMENTAL APPLICATIONS

Several measurement campaigns have taken place at CERF starting in 1992. Many institutions from all over Europe, as well as from the USA, Canada and Japan, have used the facility to test various types of passive and active detectors. These included devices such as TEPCs, GM-counters, different types of rem counters, bubble detectors, scintillation based dose-rate meters, electronic pocket dosimeters, Si-diodes, track etched detectors (TED), thermoluminescent dosimeters (TLD), films, nuclear track detectors, recombination chambers, multisphere systems, CR-39 foils. Although most of the beam time was dedicated to test dosimetric instrumentation, the facility has also been exploited for other uses, such as verifying the effect of radiation on computer memories and testing prototypes of a beam loss monitor for the future CERN Large Hadron Collider (LHC). As mentioned above, all instruments and

dosemeters used for on-board measurements in the framework of the EU funded programmes have been periodically tested and calibrated at CERF<sup>(3)</sup>. In addition, several other institutions have performed various types of measurements at the facility over the years. To demonstrate the range of applications of CERF, this section gives a (possibly non-exhaustive) overview of the most important experimental applications for which the facility has been used. This overview groups, somehow arbitrarily, the investigations in the following categories: test and intercomparison of either active instrumentation or passive devices, active and passive dosemeters used for individual monitoring, in-flight measurements based on CERF calibration either on commercial flights or in space, tests related to the LHC project, investigations of computer memory upsets and radiobiological studies. A few representative experimental results are reported.

### Active instrumentation

A first intercomparison of the response of dosemeters used in high-energy stray radiation fields was carried out in 1992 at the “pre-CERF” facility. At that time the facility had not yet the present configuration. The beam used was 200 GeV/c positive hadrons (2/3 protons and 1/3 positive pions) and the target assembly consisted of an iron block 140 cm long, 50 cm wide and 30 cm high. Top shielding, where measurements were performed, was either 80 cm thick concrete or 60 cm thick iron. Measurements were also made in front of the access door to check the dosimeter response in a softer field. The instruments tested were different TEPCs, conventional and extended range rem counters, a recombination chamber type REM-2<sup>(38)</sup> (a cylindrical, parallel-plate ionisation chamber with 25 tissue-equivalent electrodes, manufactured in Poland. It has a volume of 2000 cm<sup>3</sup>, mass of 6 kg and an effective wall thickness of 2 g/cm<sup>2</sup>; it is filled with a mixture of methane and nitrogen (5%) at a pressure of about 1 MPa), the CERBERUS (a multiple-detector system, developed at CERN, consisting of a rem ionisation chamber, a tissue-equivalent ionisation chamber, an air-filled aluminium chamber and a <sup>11</sup>C activation detector), a set of Bonner spheres and NTA films<sup>(46)</sup>.

Golnik and co-workers have investigated the application of recombination chambers in the determination of microdosimetric data, based on the comparison of saturation curves measured for mixed radiation with those for reference gamma radiation (<sup>137</sup>Cs). Measurements performed in the CERF field showed that the low-LET component predominates in the absorbed dose, on both the concrete and iron roof-shields and equals 90% for the former and 73% for the latter. These values are in good agreement with the results of measurements with the HANDI TEPC in use at CERN<sup>(47)</sup>. The values of ambient dose equivalent rate obtained by different types of recombination chambers compared well with those from other devices<sup>(48)</sup>. In particular, a REM-2 recombination chamber was used to investigate the low-LET background radiation, as discussed above<sup>(38)</sup>.

The responses of various types of rem counters were compared on the concrete roof-shield in a dedicated experiment. Two of the instruments were of conventional design and four were cylindrical or spherical versions of the LINUS. The results, given in Table 3 together with values measured by the CERN HANDI TEPC, showed a good agreement amongst the various LINUS. The two conventional rem counters underestimated the total dose equivalent by about 40%, due to their reduced response above 20 MeV. This result was found in perfect agreement with previous measurements with high energy neutrons<sup>(26-28,49)</sup>. The value of ambient dose equivalent for the several LINUS was also found in remarkable agreement with that measured by the TEPC<sup>(50)</sup>.

Lindborg and co-workers have developed the “Sievert-instrument”, a device consisting of two TEPCs with diameter of 11.5 cm simulating mean chord lengths of 2 μm, and electronics units for analysing the signal according to the variance-covariance method. The instrument is

calibrated in  $H^*(10)$  in a  $^{137}\text{Cs}$  field and its response to broad neutron fields was investigated at the CERF facility. With the assumption that the LET distribution in the atmosphere is reasonably well characterised by a combination of a CERF field and a low-LET field, the instruments can be used directly for measurements on-board <sup>(51,52)</sup>.

**Table 3.** Comparison of the response of rem counters in position 6 of the concrete roof-shield of CERF. The reference values measured by the CERN HANDI TEPC spectrometer are also given. The total uncertainty includes the statistical uncertainty on detector counts and the 10% uncertainty on the PIC-counts.

Detector	Calibration		Ambient dose equivalent	
	Factor (nSv/cts)	Procedure	(nSv/PIC)	Total uncertainty
Studsvik (CERN)	0.98	$H^*(10)$ , PuBe source	0.145	$1.64 \times 10^{-2}$
Berthold (CERN)	0.353	$H^*(10)$ , PuBe source	0.148	$1.49 \times 10^{-2}$
Cylindrical LINUS (CERN)	1.49	$H^*(10)$ , PuBe source	0.262	$2.95 \times 10^{-2}$
Spherical LINUS (CERN)	0.92	$H^*(10)$ , PuBe source	0.243	$2.77 \times 10^{-2}$
Spherical LINUS (Univ. Mi)	0.776	$H^*(10)$ , AmBe source	0.228	$2.49 \times 10^{-2}$
Cylindrical LINUS (NRPB)	1.11	$H^*(10)$ , AmBe source	0.247	$2.5 \times 10^{-2}$
TEPC ICRP21			0.242	$3.0 \times 10^{-2}$
ICRP60			0.273	$2.7 \times 10^{-2}$

### Passive dosimetry

Spurny and Bottolier-Depois have investigated at CERF three microdosimetry methods based on a TEPC, on chemically etched polyallyldiglycolcarbonate (PADC) solid state nuclear track detectors and on bubble detectors, respectively. A LET spectrometer has been developed based on PADC. The microdosimetric spectra determined on-board aircraft and behind the shielding of high-energy particle accelerators were compared. The spectra obtained with the NAUSICAA TEPC and with the PADC LET spectrometer agree well; their form is similar in the CERF reference field and on-board aircraft. Bubble detectors were tested at CERF and on-board aircraft, to verify their relative response with different thresholds in different radiation fields <sup>(53)</sup>.

The extension of the response of bubble detectors to high-energy neutrons was experimentally determined at CERF by exposing the dosimeters inside lead converters of various thicknesses. Monte Carlo calculations were performed to assess the effect of the lead converter on the neutron spectral fluence. The experimental results were compared with the calculated ambient dose equivalent obtained by folding the response of the detectors with the modified neutron spectrum. Both the experimental and the Monte-Carlo results indicated that the dosimeter can be made to respond correctly to neutron energies above 20 MeV; the required

lead thickness is 1 cm to 1.5 cm. It has also been shown that this additional material does not perturb the detector response to lower energy neutrons <sup>(54)</sup>.

CR-39 nuclear track detectors have been employed on a number of subsonic and supersonic aircraft to measure charge spectra and LET spectra at cruising altitudes. In order to test the overall validity of the technique, measurements were carried out at the CERF facility and good agreement was found with dose values obtained using mainly heavy ion calibration <sup>(55)</sup>.

### Individual monitoring

Spurny has tested several individual dosimeters for both the low-LET and high-LET components in high-energy radiation reference fields at JINR (Dubna, Russia) and at CERF as well as on-board aircraft during commercial flights. Three types of electronic personal dosimeters based either on Si-diodes or on a small GM-counter and several passive dosimeters (TLDs, Al-P glass and photographic films) were used for the low-LET component. For the high-LET component, nuclear emulsions, albedo dosimeters, TED in contact with fissile radiators, PADC TED and two types of bubble detectors were investigated <sup>(56)</sup>. The relative response of the high-LET dosimeters is shown in Table 4. The response of Czech routine personal dosimeters in high-energy radiation reference fields was also investigated at JINR and at CERF. The study has demonstrated that the values obtained through the routine interpretation procedure never lead to an underestimation of exposure but rather to a large (up to a factor of 5) overestimation. If information on the neutron spectrum is available for the interpretation of the dosimeter reading, the agreement of values obtained by means of the routine neutron dosimeter and reference values becomes quite satisfactory <sup>(57)</sup>.

**Table 4.** Relative response of individual dosimeters to the high-LET component of CERF <sup>(56)</sup>.

Dosimeter	Relative response of dosimeter to TEPC	
	Concrete roof-shield	Iron roof-shield
<sup>6</sup> LiF in albedo PGP DIN	0.10 ± 0.02	0.40 ± 0.09
Nuclear emulsion NTA	3.70 ± 0.90	1.50 ± 0.30
TED with fissile radiators	2.90 ± 0.50	1.60 ± 0.20
TED PADC	0.35 ± 0.06	0.26 ± 0.04
BDND BD 100R	0.57 ± 0.09	1.35 ± 0.18
BDND PND	0.63 ± 0.11	1.49 ± 0.21
SDD 100	0.59 ± 0.11	0.66 ± 0.09
SDD 1000	0.77 ± 0.15	0.27 ± 0.06
SDD 6000	1.14 ± 0.20	0.24 ± 0.05

An intercomparison of personal dosimeters from seven US accelerator facilities (ANL, BNL, LBNL, LANL, PNNL, SLAC and TJNAF) was conducted at CERF. Part of the dosimeters shipped to CERN were exposed at CERF, part to neutrons from a <sup>238</sup>Pu-Be( $\alpha$ ,n) source and part were used as controls to correct for background radiation encountered during transit to and from CERN. The following types of dosimeters were investigated: Panasonic

model 810 ( ${}^6\text{Li}_2{}^{10}\text{B}_4\text{O}_7$  and  ${}^7\text{Li}_2{}^{11}\text{B}_4\text{O}_7$ ) plus CR-39; Harshaw model 8816 neutron TLD (TLD-700 plus TLD-600)/TED; Harshaw model 8825 beta-gamma TLD 700; Harshaw model 8814 TLD ( ${}^7\text{LiF:Mg,Ti}$  and  ${}^6\text{LiF:Mg,Ti}$ ) plus CR-39 TED detector; CR-39 TED in various forms and submitted to different etching procedures; Panasonic model UD-802 using lithium tetraborate ( $\text{LiBO}_4$ ) or  $\text{Li}_2\text{B}_4\text{O}_7\text{:Cu}$  and calcium sulphate ( $\text{CaSO}_4$ ) or  $\text{CaSO}_4\text{:Tm}$ . The experiment showed that if a field-specific calibration factor is used to correct the dose equivalent responses, the agreement with the reference dose equivalent for all the dosimeters is better than about 25 to 65% <sup>(58)</sup>.

A Japanese group has developed a real-time neutron personal dosimeter, which contains a fast and a slow neutron sensor. Both sensors are p-type silicon semiconductor detectors, the latter with a natural boron layer deposited around an aluminium electrode to detect  $\alpha$  and Li ions from the  ${}^{10}\text{B}(\text{n}, \alpha)$  reaction. A thin polyethylene radiator is in contact with the front surface of each sensor to produce recoil protons. Field measurements of the performance of the device were carried out around several nuclear facilities (reactors, accelerators and nuclear fuel handling facilities) including CERF (both on the concrete and iron roof-shields). The dosimeter is now commercially available from Fuji Electric Co. Ltd <sup>(59)</sup>.

### **On-flight measurements based on CERF calibration**

Measurements were performed on Concorde using the NRPB (U.K.) passive survey meter, which uses 30 to 40 dosimeters for both the neutron and non-neutron component of the field. The survey meter uses dosimeters from the NRPB routine personal dosimetry services (TLDs for the non-neutron component and PADC TEDs for the neutron component). A calibration factor was determined for the neutron fluence response of the passive survey meter for the CERF concrete roof-shield. Both batch and sheet dependence of this calibration factor have been investigated. It was concluded that a sheet and batch calibration factor can be applied, but a periodic check should be made. The results are given in Figure 7. It is assumed that the fluence response measured for the CERF spectrum can be corrected by the ratio of the predicted responses of the passive survey meter for the calculated neutron spectrum in the atmosphere by Heinrich et al <sup>(60)</sup> to that calculated for CERF. The use of the CERF calibration is considered to give a good estimate, within 20 or 30% systematic uncertainty, of effective dose or ambient dose equivalent for the neutron component of the cosmic radiation field in aircraft <sup>(12)</sup>.

As part of a continuing assessment of the cosmic radiation exposure of Canadian-based aircrew, a TEPC was used to take dosimetric measurements on-board 64 flights from September 1998 to October 1999. In conjunction with the in-flight measurements, the operation of the TEPC was verified using several common radioisotopic sources and in the CERF neutron field. The values of various microdosimetric quantities obtained from several terrestrial sources, including those obtained from the CERF spectrum, provided a useful comparison to the values obtained from the radiation field at jet altitudes <sup>(61)</sup>.

A diverse array of both passive and active instruments, to cover all radiation components of the field at aviation altitudes, was employed in the Italian national survey of aircrew exposure <sup>(10)</sup>. The detectors used were: the LINUS; the ANPA stack, a passive multidetector stack including bubble detectors (for low-energy neutrons), bismuth-fission track detectors (for high-energy neutrons), cellulose nitrate (LR-115 from Kodak) and polycarbonate films for high-Z particles, and various TLDs (including the hypersensitive Chinese lithium fluoride GR-200) for the low-LET component; the DIAS stack consisting of 20 sheets of CR-39 used to determine the fluence and type of charged particles as well as their LET; TEPC; PADC (CR-39); a high-pressure ionisation chamber Reuter-Stokes type RSS-112 (based on a spherical stainless steel ionisation chamber filled with ultra-pure argon gas under high pressure). All these dosimetric



systems have provided consistent results when exposed together at CERF <sup>(62)</sup>. An example of the agreement obtained between the range of instruments employed is shown in Table 5 <sup>(15)</sup>.

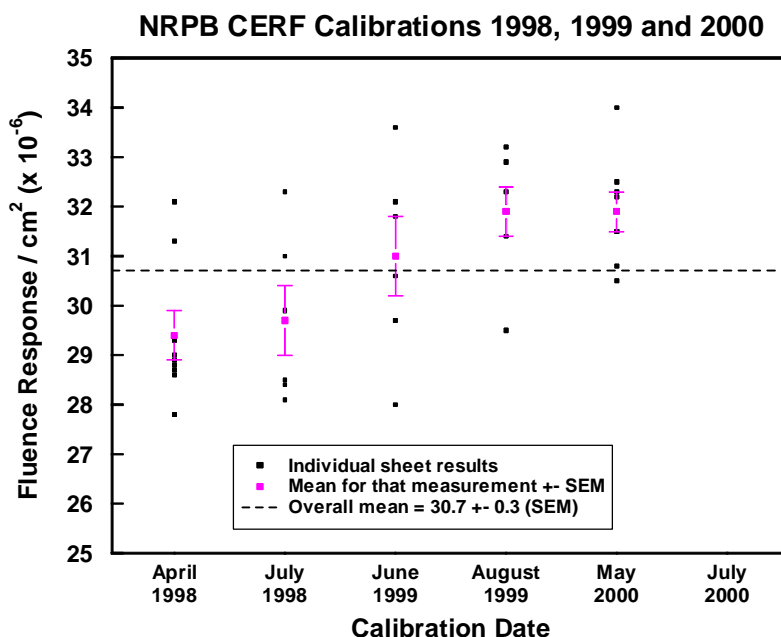


**Fig. 7.** Calibration measurements of the NRPB passive survey meter, PADC neutron detectors at CERF (April 1998 to July 2000) <sup>(12)</sup>.

**Table 5.** Measured and calculated ambient dose equivalent rates at CERF relative to the CERN HANDI TEPC (high-let component > 6 keV/μm) <sup>(15)</sup>.

FLUKA calculated/CERN TEPC	0.91 ± 0.07 (a)
USAAR HANDI/CERN TEPC	0.88 and 1.02
ANPA stack/CERN TEPC	0.95 ± 0.1
NRPB etched track (predicted)/ CERN TEPC	1.2 ± 0.1
DIAS etched track/CERN TEPC	1.18 ± 0.12

(a) Average over all 16 concrete roof-shield locations

### Measurements related to space programmes

CERF has also been used to test instrumentation flown in space. The response of a space shuttle TEPC was investigated at the facility and compared to other dosimetric devices <sup>(63)</sup>. When exposed to high-energy neutrons, the dose equivalent response was found nearly the same as that of the HANDI TEPC of CERN. Over the LET range produced primarily by charged particles (< 20 keV/μm) the response of the TEPC is nearly identical to that of the DOSTEL telescope, consisting of two 300 μm thick Si detectors, developed at the University of Kiel <sup>(64)</sup>.

A new active personal neutron dosimeter developed at PTB for use in the space station MIR and the space shuttle, based on silicon diodes, shows improved sensitivity to neutrons, rejects

charged particles by anticoincidence and, in addition, gives information on the neutron spectrum. It consists of a stack of silicon detectors sandwiched between layers acting as neutron converters, moderators and absorbers. A response matrix has been determined by measurements in monoenergetic neutron reference fields. The first results of measurements at CERF showed good agreement with energy distributions calculated by the FLUKA code <sup>(65)</sup>. The above active device was further developed for measuring the energy and directional distribution of neutron fluence in fields of broad energy spectra and with a high background of photon and muon radiation. Six detector capsules were mounted on a 30 cm diameter polyethylene sphere, each of them containing four silicon detectors with different converters and shields. The energy and directional distribution of the fluence is reconstructed from the pulse height spectra and from the response function determined with monoenergetic neutron fields. The dose equivalent measured with the spectrometer agrees within 25% of the reference value. The results show that this directional spectrometer provides reasonable results in fields with wide energy distributions, even in the case of intense low-LET background as in CERF <sup>(66,67)</sup>.

### **Applications related to the LHC project**

As mentioned above, the facility is also used for applications other than dosimetry. A CERN group has made preliminary measurements with microcalorimeters in view of their possible use as beam-loss monitors for the LHC. A carbon resistance, acting as a thermometer, is thermally coupled to a copper block, initially at the cryostat temperature. As a result of high-energy particle losses the resulting shower deposits heat into the copper. The measurement of the resistance decrease as a result of the copper temperature increase is expected to provide a means of estimating the number of lost particles. A small cryostat vessel coupled to a 100 litre He dewar was built. The cryostat provides the required temperature of about 1.9 K to the calorimeters placed inside under a vacuum pressure lower than  $10^{-4}$  Pa. The device was tested with different microcalorimeters in the laboratory and directly in the hadron beam at the CERF facility. The time response of the calorimeters to a hadron spill on target was determined. A good relationship was found between the amount of "lost" particles and the change of the thermometer resistance, for a beam intensity varying by a factor of 10 <sup>(68)</sup>.

There is also a collaboration with the ATLAS muon background group of CERN. In summer 1999 a benchmark of the ATLAS background situation was carried out at CERF. A cast iron construction, irradiated by the hadron beam, was used to verify the reliability of the FLUKA code under ATLAS conditions. The chosen set-up can be seen as an analogue to the ATLAS forward calorimeter, not only in terms of hadronic absorption lengths, but also in several other respects. Particles with ATLAS relevant energies hit the absorber and produced hadronic and electromagnetic showers. A measurement set-up based on a BGO detector was installed behind the iron absorber, to measure the energy deposition induced by the produced particle showers. This scenario is similar to the expected photon and neutron background at the location of the ATLAS muon chambers. The results of the benchmarking showed that the simulations are in good agreement with the experimental data. With respect to the ability of FLUKA to calculate shower processes it was demonstrated that the uncertainty factor of 5 used until then could be reduced to 1.2 <sup>(69)</sup>.

### **Computer memory upsets**

Heinrich has included measurements at CERF in his study of neutron-induced Single Event Upsets (SEU) in Static Random Access Memories (SRAMs). SRAMs were exposed to the radiation in the upper atmosphere during dedicated flights, during some commercial flights and to radiation fields at different particle accelerators: protons at PSI (Villigen, Switzerland),

180 MeV neutrons at Uppsala (Sweden) and at the CERF facility in April 1998 and in June 1999. Experiments at the accelerator facilities have supported some fundamental data with high statistical significance. Data collected on different flights are in good agreement with predictions based on the accelerator results and calculated neutron fluence at flight levels <sup>(70)</sup>.

## **Radiobiology**

A radiobiological investigation was also conducted at CERF, in spite of the lack of supporting structure at CERN for this type of application. Heimers has determined the RBE of a mixed neutron-gamma simulated cosmic radiation field and its high-LET component, on the induction of chromosome aberrations in human lymphocytes. The results of this preliminary investigation showed a high RBE of cosmic radiation and its neutron component in comparison with <sup>60</sup>Co gamma radiation - up to 64, and up to 113 when calculating only the high-LET component <sup>(71)</sup>.

Other experimental results obtained at CERF are reported in the literature <sup>(72-78)</sup>.

## **LATEST DEVELOPMENTS**

In a space station neutrons make an important contribution to the personal dose equivalent. Most of the neutrons inside the station result from nuclear interactions of the charged particles (mainly galactic protons and protons trapped by the earth's magnetic field) with the wall material of the vessel. A plot of  $E \cdot \Phi(E)$  against  $\log(E)$ , where  $\Phi(E)$  is the neutron fluence, shows peak intensities at about 1 MeV and 100 MeV, while for protons the peaks show at about 100 MeV (trapped proton source) and in the GeV region (galactic proton source). In fact, as mentioned in the previous section, for the evaluation of dosimeters used in space the calibration value determined at CERF was taken for fast neutrons because this field is considered to be most similar to that in space.

Nevertheless, several other particles contribute to the dose in a space station or in a shuttle orbiting around the earth, or in a spacecraft travelling, for example, to Mars. Also, astronauts performing extravehicular activities are directly exposed to the cosmic ray field. It was thus decided to study whether a different shielding configuration at CERF could produce a more complex radiation field, rich in high-energy particles, which could be of interest for forthcoming measurements in the framework of the space programme. Preliminary Monte-Carlo simulations were performed with the FLUKA code <sup>(22,23)</sup> to investigate this possibility. To avoid unnecessary time-consuming calculations, simulations were carried out in a simplified spherical geometry (Figure 8) rather than modelling the complete facility. The aim was to understand if a given target/shielding combination and angular scoring region would indicate a promising situation which could subsequently be investigated more thoroughly. Eventually, the actual facility will have to be properly modelled. Calculations were performed for the "standard" 50 cm thick, 7 cm diameter copper target as well as for smaller targets, one 10 cm long and 7 cm in diameter, another 10 cm long and 1 cm in diameter. The study aims to produce a radiation field mainly rich in high-energy protons similar to that found in the stratosphere <sup>(79)</sup> or high-energy neutrons and other secondary particles as found inside the space station or a spacecraft <sup>(80)</sup>. The intention is also to increase the available dose equivalent rate at the exposure locations.

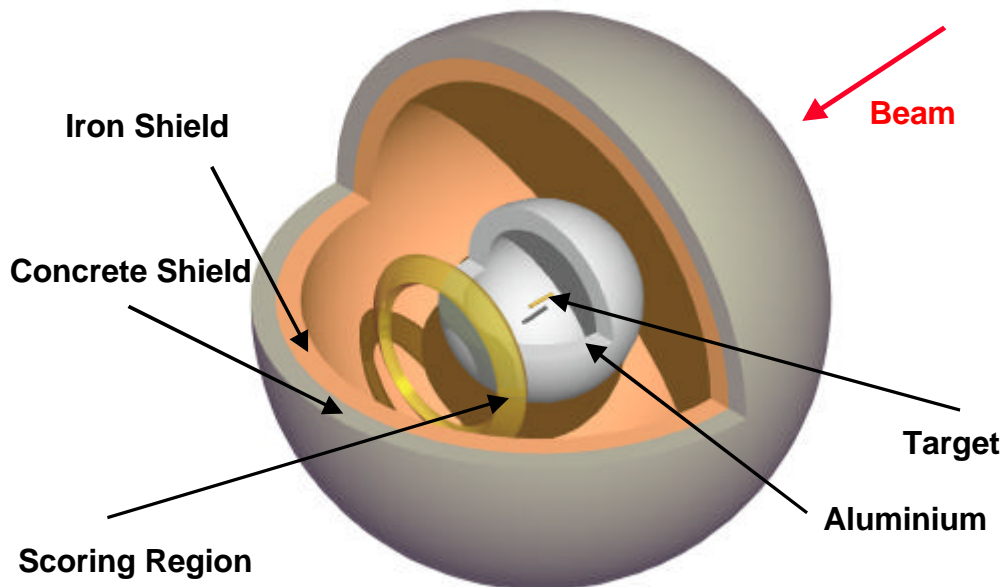


**Fig. 8.** *Simplified spherical geometry used for the preliminary calculations for the upgrade of the CERF facility for reproducing the radiation field in a space vessel.*

First, calculations were made for the “standard” hadron beam incident on the target, i.e. a mixed beam composed of one third protons and two third positive pions of 120 GeV/c momentum. The target was at the centre of a spherical shield, with scoring done in conical regions 10° wide (0° to 90°). Neutrons, protons, pions, muons, photons and electrons were scored. A 10 cm thick aluminium shield was placed at either 1 m or 1.2 m distance from the target. Since in a practical situation the dose equivalent rate produced by such configuration will be much higher than that presently available at CERF, the reference exposure area will have to be shielded. An additional layer of material acting as back shield was therefore included in the simulations, made up of either 80 cm thick concrete placed at 2 m distance from the aluminium layer, or 40 cm iron backed by 40 cm concrete placed at 2.5 m distance from the aluminium. The most interesting results were obtained with the “standard” copper target and the latter shielding configuration described above. The particle spectra in the forward direction (0° to 10° angular region) are shown in Figure 9.

A simulation made without the back shield showed that this shield is responsible for the low-energy neutron component shown in the figure. One should note, in particular, that the high-energy component (above 100 MeV) of the proton spectrum is similar to the energy spectrum of cosmic ray protons <sup>(79)</sup>. Also, the neutron energy distribution extends up to about 100 GeV versus a few hundreds MeV of the present CERF configuration on the concrete roof shield. The neutron fluence is about  $6.5 \times 10^{-3} \text{cm}^{-2}$  and  $4.3 \times 10^{-3} \text{cm}^{-2}$  per primary particle on the copper target, in the forward (0°-10°) and transverse (80°-90°) directions, respectively, as compared to the present figure of  $3.5 \times 10^{-5} \text{cm}^{-2}$ . On the other hand, the pion component is too high in comparison to that present in space. This configuration has the advantage that an independent exposure area could in principle be built and run in parallel to the present set-up (i.e. simultaneous data taking on the concrete roof-shield or on the iron roof-shield). Another series of simulations were performed with increasing aluminium thickness, aiming at reducing the pion component relative to the other particles. Figure 10 shows the results with 40 cm aluminium at 30°-40° emission angle, where it is actually seen that the pion component decreases with respect to neutrons with increasing aluminium thickness and emission angle.

With 80 cm aluminium the pion as well as the photon component further decrease (Figure 11). To compare the spectral fluences produced by graphite instead of aluminium, a simulation was performed with a 40 cm graphite shield and 205 GeV/c beam. Both the pion and the photon component slightly increase, so that this material brings no advantages with respect to aluminium. The configuration yielding the spectral distributions shown in Figure 11 is thus considered to be the best choice.

The influence of primary beam momentum on the produced secondary particles was investigated in the range 40-400 GeV/c. The simulations were performed with the actual particle composition of the SPS beams. These are made up of about 85% pions and 15% protons at 40 GeV/c, 2/3 pions and 1/3 protons at 120 GeV/c, 1/3 pions and 2/3 protons at 205 GeV/c and protons only at 400 GeV/c. It turned out that the spectral shape and the secondary particle composition do not change much with beam momentum, but the absolute fluence per beam particle on target increases by about a factor of 2 by raising the momentum from 205 to 400 GeV/c and by a factor of 7 from 40 to 400 GeV/c. With increasing emission angle the neutron component becomes more and more dominant. As an example, Figure 12 shows the particle spectra for 205 GeV/c and 60°-70° emission angle.

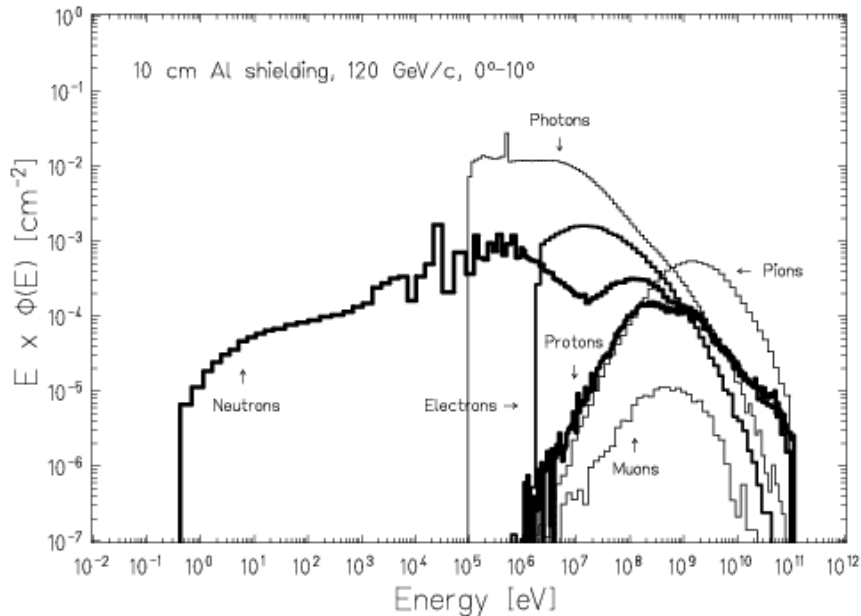


**Fig. 9.** Particle spectral fluences (lethargy) in the 0°-10° angular region for a positive 120 GeV/c beam (particles per primary beam particle incident on the target). The target is copper, 50 cm thick and 7 cm in diameter; 10 cm thick aluminium shield placed at 1 m from the target; external shielding is 40 cm iron backed by 40 cm concrete placed at 2.5 m distance from the aluminium slab.

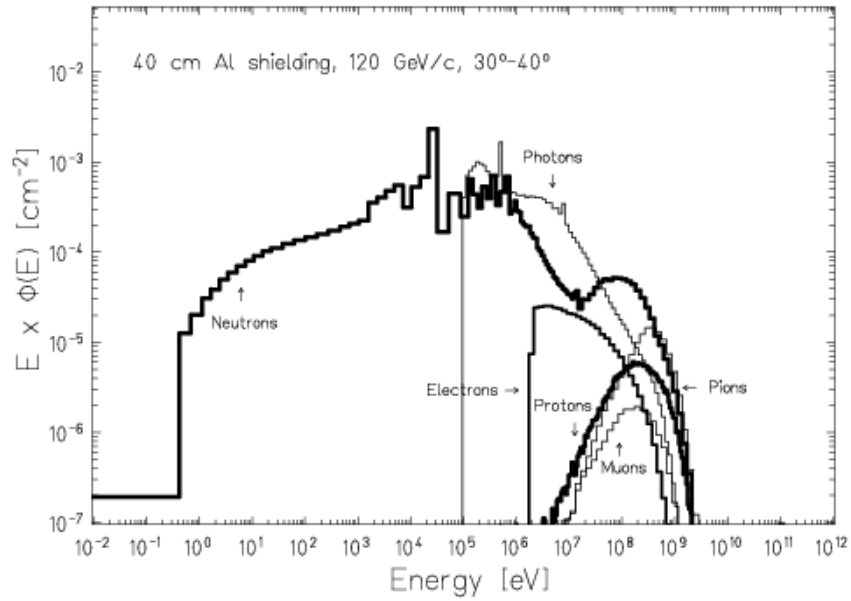


**Fig. 10.** Particle spectral fluences (lethargy) in the 30°-40° angular region for a positive 120 GeV/c beam (particles per primary beam particle incident on the target). The target is copper, 50 cm thick and 7 cm in diameter; 40 cm thick aluminium shield placed at 1 m from the target; external shielding is 40 cm iron backed by 40 cm concrete placed at 2.5 m distance from the aluminium slab.

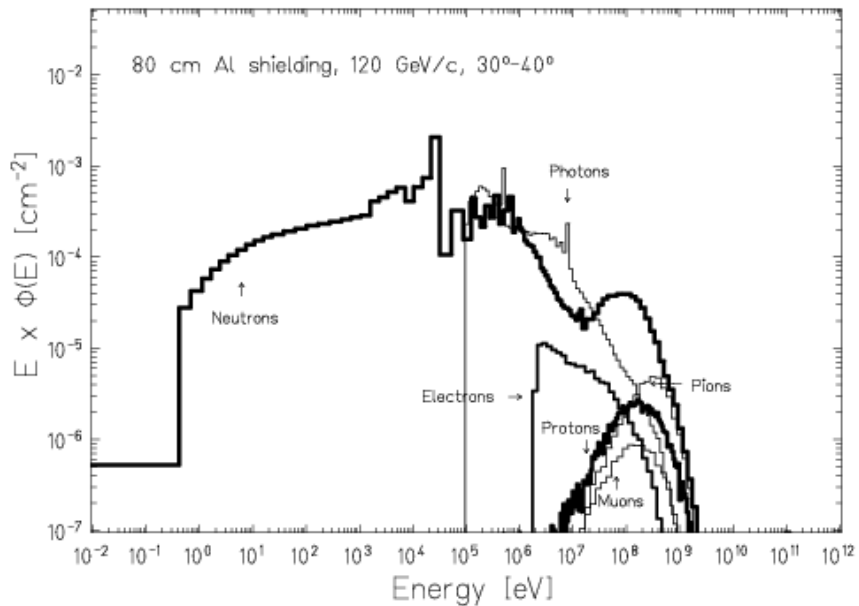


**Fig. 11.** Particle spectral fluences (lethargy) in the 30°-40° angular region for a positive 120 GeV/c beam (particles per primary beam particle incident on the target). The target is copper, 50 cm thick and 7 cm in diameter; 80 cm thick aluminium shield placed at 1 m from the target; external shielding is 40 cm iron backed by 40 cm concrete placed at 2.5 m distance from the aluminium slab.

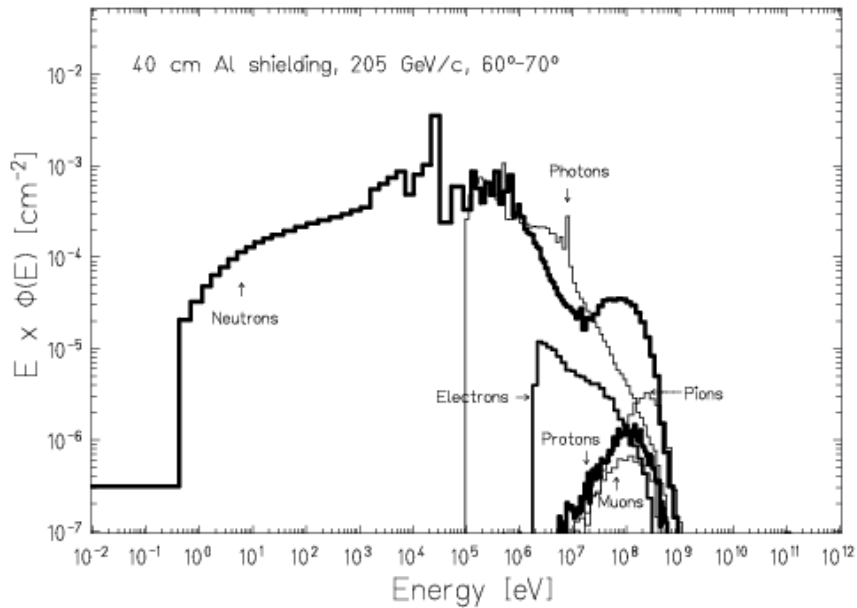


**Fig. 12.** Particle spectral fluences (lethargy) in the  $60^\circ$ - $70^\circ$  angular region for a positive 205 GeV/c beam (particles per primary beam particle incident on the target). The target is copper, 50 cm thick and 7 cm in diameter; 40 cm thick aluminium shield placed at 1 m from the target; external shielding is 40 cm iron backed by 40 cm concrete placed at 2.5 m distance from the aluminium slab.

## CONCLUSIONS

The calibration of instruments and dosimeters at CERF is expected to continue to play an important role in the fourth EU funded programme on the investigation of radiation fields and dosimetry at aviation altitudes which has just started. There is also an increasing interest by many research institutions outside the EU collaboration in using the facility, including measurements in the framework of the space programme. All these factors should guarantee the healthy operation of CERF in the next few years, despite the competition for beam time at the SPS from the large LHC collaborations. Promising Monte Carlo results have been obtained in view of extending the range of particle spectra provided at CERF. These preliminary results will have to be confirmed by more accurate calculations, but an upgrade of the facility is conceivable with a comparatively limited effort. Applications for beam time at CERF can be addressed to one of the authors (MS, e-mail: marco.silari@cern.ch).

## ACKNOWLEDGEMENTS

The operation of CERF is partially supported by the European Commission, Directorate General XII, contracts no. F13P-CT92-0026 (1992-1995), F14P-CT95-0011 (1996-1999) and FIGM-CT-2000-00068 (the present contract). A. Fassò, M. Höfert, T. Otto, G.R. Stevenson and L. Ulrici have contributed substantially to the set-up, start-up and operation of the facility over the past years. Early Monte Carlo calculations were performed by G.R. Stevenson, the most recent ones by A. Ferrari, E. Nava and T. Rancati. In particular we wish to thank A. Ferrari for many useful discussions and T. Rancati for providing the data of Table 2. Figure 1 was taken from ref. (3), for which we wish to thank H. Schraube and D. O'Sullivan. We also wish to thank D. Bartlett for providing us with the latest results of the NRPC PADC calibration appearing in Figure 7.

## References

- 1 International Commission on Radiological Protection. *1990 Recommendations of the International Commission on Radiological Protection*. ICRP Publication 60 (Oxford: Pergamon Press) (1990).
- 2 Council Directive 96/29/Euratom of 13 May 1996. *Laying down basic safety standards for the protection of the health of workers and the general public against the dangers arising from ionizing radiation*. Official Journal of the European Communities L159, Volume 39, 1-114 (29 June 1996).
- 3 *Study of radiation fields and dosimetry at aviation altitudes*. EU contract number F14P-CT950011, Final report, January 1996-June 1999, Report DIAS 99-9-1, Dublin Institute for Advanced Studies, Dublin, Ireland (1999).
- 4 Beck, P., Schrewe, U., O'Brien, K. and Ambrosi, P. *ACREM, air crew radiation exposure monitoring*. Report OEFZS-G-0008, Austrian Research Centres Seibersdorf (November 1999).
- 5 Bartlett, D.T., Grillmaier, R., Heinrich, W., Lindborg, L., O'Sullivan, D., Schraube, H., Silari, M. and Tommasino, L. *The cosmic radiation exposure of aircraft crew*. Proceedings of Conference - 11<sup>th</sup> International Congress of Radiation Research, Dublin (Ireland), 18-23 July 1999, Radiation Research, Volume 2: Congress Proceedings, edited by Moriarty, M., Mothersill, C., Seymour, C., Edington, M., Ward, J.F. and Fry, R.J.M. Allen Press, Inc., 719-723 (2000).
- 6 Menzel, H-G., O'Sullivan, D., Beck, P. and Bartlett, D. *European measurements of aircraft crew exposure to cosmic radiation*. Health Phys. **79**, 563-567 (2000).
- 7 European Radiation Dosimetry Group. *Exposure of air crew to cosmic radiation*. EURADOS Report 1996-01, edited by McAulay, I.R., Bartlett, D.T., Dietze, G., Menzel, H.G., Schnuer, K., Schrewe, U.J. (1996).
- 8 Schrewe, U.J. *Global measurements of the radiation exposure of civil air crew from 1997 to 1999*. Radiat. Prot. Dosim. **91**, 347-364 (2000).
- 9 Lewis, B.J., Tume, P., Bennet, L.G.I., Pierre, M., Green, A.R., Cousins, T., Hoffarth, B.E., Jones, T.A. and Brisson, J.R. *Cosmic radiation exposure on Canadian-based commercial airline routes*. Radiat. Prot. Dosim. **86**, 7-24 (1999).
- 10 Curzio, G., Grillmaier, R.E., O'Sullivan, D., Pelliccioni, M., Piermattei, S. and Tommasino, L. *The Italian national survey of aircrew exposure: II. On-board measurements and results*. Radiat. Prot. Dosim. **93**, 125-133 (2001).
- 11 Townsend, L.W., editor. Proceedings of Conference - 34<sup>th</sup> Annual Meeting of the National Council on Radiation Protection and Measurements: Cosmic Radiation Exposure of Airlines Crews, Passengers and Astronauts. Health Phys. **79**, 470-613 (2000).



- 12 Bartlett, D.T., Hager, L.G., Irvine, D. and Bagshaw, M. *Measurements on Concorde of the cosmic radiation field at aviation altitudes*. Radiat. Prot. Dosim. **91**, 365-376 (2000).
- 13 Beaujean, R., Kopp, J. and Reitz, G. *Radiation exposure in civil aircraft*. Radiat. Prot. Dosim. **85**, 287-290 (1999).
- 14 Alberts, W.G., Alevra, A.V., Ferrari, A., Otto, T., Schrewe, U.J. and Silari, M. *Calibration problems, calibration procedures and reference fields for dosimetry in flight altitudes*. Radiat. Prot. Dosim. **86**, 289-295 (1999).
- 15 O'Sullivan, D., Bartlett, D., Grillmaier, R., Heinrich, W., Lindborg, L., Schraube, H., Silari, M., Tommasino, L. and Zhou D. *Investigation of radiation fields at aircraft altitudes*. Radiat. Prot. Dosim. **92**, 195-198 (2000).
- 16 Russ, J.S., Stevenson, G.R., Fassò, A., Nielsen, M.C., Furetta, C., Rancoita, P.G. and Vismara, L. *Low-energy neutron measurements in an iron calorimeter structure irradiated by 200 GeV/c hadrons*. CERN Divisional Report TIS-RP/89-02 (1989).
- 17 Fassò, A., Stevenson, G.R., Bruzzi, M., Furetta, C., Rancoita, P.G., Giubellino, P., Steni, R. and Russ, J.S. *Measurements of low-energy neutrons in an iron calorimeter structure irradiated by 24 GeV/c hadrons*. CERN Divisional Report TIS-RP/90-19 (1990).
- 18 Stevenson, G.R., Fassò, A., Furetta, C., Rancoita, P.G., Giubellino, P., Russ, J.S. and Bertrand, C. *Measurements of low-energy neutrons in a lead calorimeter structure irradiated by 200 GeV/c hadrons*. CERN Divisional Report TIS-RP/91-11 (1991).
- 19 Fassò, A., Ferrari, A., Ranft, J., Sala, P.R., Stevenson, G.R. and Zazula, J.M. *A comparison of FLUKA simulations with measurements of fluence and dose in calorimeter structures*. Nucl. Instrum. and Meth. A **332**, 459-468 (1993).
- 20 Höfert, M. and Stevenson, G.R. *The CERN-CEC high-energy reference field facility*. Proceedings of Conference - 8<sup>th</sup> International Conference on Radiation Shielding, Arlington, Texas, April 1994. American Nuclear Society, Inc., 635-642 (1994).
- 21 Birattari, C., Ferrari, A., Höfert, M., Otto, T., Rancati, T. and Silari, M. *Recent results at the CERN-EC high-energy reference field facility*. Proceedings of Conference - Satif-3 Shielding Aspects of Accelerators, Targets and Irradiation Facilities, Sendai, Japan 1997. NEA/OECD, 219-234 (1998).
- 22 Fassò, A., Ferrari, A., Ranft, J. and Sala, P.R. *New Developments in FLUKA modelling of hadronic and EM interactions*. Proceedings of Conference - Simulating Accelerator Radiation Environments (SARE3), Tsukuba, Japan, May 1997. Edited by Hirayama, H. KEK Proceedings 97-5, 32-44 (1997).
- 23 Ferrari, A., Rancati, T. and Sala, P.R. *FLUKA application in high-energy problems: from LHC to ICARUS and atmospheric showers*. Proceedings of Conference - Simulating Accelerator Radiation Environments (SARE3), Tsukuba, Japan, May 1997. Edited by Hirayama, KEK Proceedings 97-5, 165-176 (1997).

- 24 Birattari, C., De Ponti, E., Esposito, A., Ferrari, A., Magugliani, M., Pelliccioni, M., Rancati, T. and Silari, M. *Measurements and simulations in high-energy neutron fields*. Proceedings of Conference - Satif-2 Shielding Aspects of Accelerators, Targets and Irradiation Facilities, Geneva, Switzerland, October 1995. OECD/NEA, 171-197 (1996).
- 25 Birattari, C., Ferrari, A., Nuccetelli, C., Pelliccioni, M. and Silari, M. *An extended range neutron rem counter*. Nucl. Instrum. Meth. **A 297**, 250-257 (1990).
- 26 Birattari, C., Esposito, A., Ferrari, A., Pelliccioni, M. and Silari, M. *A Neutron survey meter with sensitivity extended up to 400 MeV*. Radiat. Prot. Dosim. **44**, 193-197 (1992).
- 27 Birattari, C., Esposito, A., Ferrari, A., Pelliccioni, M. and Silari, M. *Calibration of the neutron rem counter LINUS in the energy range from thermal to 19 MeV*. Nucl. Instrum. and Meth. **A 324**, 232-238 (1993).
- 28 Birattari, C., Esposito, A., Ferrari, A., Pelliccioni, M., Rancati, T. and Silari, M. *The extended range neutron rem counter 'LINUS': overview and latest developments*. Radiat. Prot. Dosim. **76**, 135-148 (1998).
- 29 Mitaroff, A. and Silari, M. *Improving the high energy response of a Bonner Sphere Spectrometer*. CERN Internal Report TIS-RP/IR/ **99-27** (1999).
- 30 Birattari, C., Cappellaro, P., Mitaroff, A. and Silari, M. *Development of an extended range Bonner Sphere Spectrometer*. Proceedings of Conference - Advanced Monte Carlo for Radiation Physics, Particle Transport Simulation and Applications, Lisbon, Portugal, October 2000 (in press).
- 31 International Commission on Radiological Protection. *Conversion coefficients for use in radiological protection against external radiation*. Publication 74 (Oxford: Pergamon Press) (1996).
- 32 Ferrari, A. and Pelliccioni, M. *Fluence to dose equivalent conversion data and effective quality factors for high energy neutrons*. Radiat. Prot. Dosim. **76**, 215-224 (1998).
- 33 Grillmaier, R.E., Gerdung, S. and Lim, T. Private communication.
- 34 Höfert, M., Sannikov, A.V. and Stevenson, G.R. *Muon background subtraction from HANDI-TEPC measurements data (CERN-CEC May 1994 experiment)*. CERN Internal Report TIS-RP/IR/**94-13** (1994).
- 35 Fassò, A., Höfert, M. and Nielsen, M. *Muon Measurements at the CERN-CEC high energy reference field facility during the H6M95 Run*. CERN Internal Report TIS-RP/IR/**95-27** (1995).
- 36 Stevenson, G.R. *Dose and dose equivalent from muons*. CERN Divisional Report TIS-RP/**099** (1983).
- 37 Otto, T. and Silari, M. *The July/August 1996 run at the CERN-CEC reference facility*. CERN Technical Memorandum TIS-RP/TM/**96-25** (1996).

- 38 Golnik, N., Silari, M. and Otto, T. *On the use of a recombination chamber for radiation measurements in CERN-EU high energy reference radiation fields*. Radiat. Prot. Dosim. **86**, 175-179 (1999).
- 39 Carlsson, A., Hooper, M.C., Liu, J., Roesler, S., Stevenson, G.R. *SL-RP Measurements during the July 1993 CERN-CEC Experiments*. CERN Technical Memorandum TIS-RP/TM/**93-32** (1993).
- 40 Hooper, M.C., Raffnsøe, C., Stevenson, G.R. *Beam Monitoring in the May 1993 CERN-CEC Experiment*. CERN Technical Memorandum TIS-RP/TM/**93-22** (1993).
- 41 Liu, J., Roesler, S., Stevenson, G.R. *Carbon-11 in beam measurements during the September 1993 CERN-CEC experiments*. CERN Technical Memorandum TIS-RP/TM/**93-43** (1993).
- 42 Roesler, S., Stevenson, G.R. *Carbon-11 measurements during the May 1994 H6 runs*. CERN Technical Memorandum TIS-RP/TM/**94-10** (1994).
- 43 Stevenson, G.R., Liu, J., O'Brian, K., Williams, J. *Beam intensity measurements using  $^{11}\text{C}$  activation for the CERN-CEC experiments*. CERN Technical Memorandum TIS-RP/TM/**94-15** (1994).
- 44 Elsener, K., Heilmann, M., Silari, M. *Verification of the calibration factor of the CERF beam monitor*. CERN Technical Memorandum TIS-RP/TM/**98-22** (1998).
- 45 Gschwendtner, E., Mitaroff, A., Ulrici, L. *A new calibration of the PIC monitor in H6*. CERN Internal Report TIS-RP/IR/**2000-09** (2000).
- 46 Birattari, C., Esposito, A., Fassò, A., Ferrari, A., Festag, J.G., Höfert, M., Nielsen, M., Pelliccioni, M., Raffnsøe, C., Schmidt, P. and Silari, M. *Intercomparison of the response of dosimeters used in high energy stray radiation fields*. Radiat. Prot. Dosim. **51**, 87-94 (1994).
- 47 Golnik, N. *Microdosimetry using a recombination chamber: method and applications*. Radiat. Prot. Dosim. **61**, 125-128 (1995).
- 48 Rusinowski, Z. and Golnik, N. *Performance tests of the IAE dose equivalent meter in radiation field of high energy calibration facility at SPS-CERN*. Nucl. Instrum. and Meth. A **408**, 600-602 (1998).
- 49 Agosteo, A., Birattari, C., Foglio Para, A., Nava, E., Silari, M. and Ulrici, L. *Neutron measurements in the stray field produced by  $158 \text{ GeV } c^{-1}$  per nucleon lead ion beams*. Health Phys. **75**, 619-629 (1998).
- 50 Silari, M. and Ulrici, L. *Intercomparison of rem counters in the CERF neutron field*. CERN Technical Memorandum TIS-RP/TM/**98-23** (1998).
- 51 Kyllönen, J-E., Lindborg L. and Samuelson, G. *Paired TEPCs for variance measurements*. In: Microdosimetry: an interdisciplinary approach. Eds. Goodhead, D., O'Neill, P. and

- Menzel, H.G., The Royal Society of Chemistry, Cambridge, Special publication No. 204 (1997).
- 52 Kyllönen, J-E., Lindborg L. and Samuelson, G. The response of the Sievert-instrument in neutron beams up to 180 MeV. *Radiat. Prot. Dosim.* (in press).
- 53 Spurny, F. and Bottolier-Depois, J.-F. *Microdosimetry of environmental radiation fields*. In: C. Baumstark-Khan et al. (eds), *Fundamentals for the Assessment of Risks from Environmental Radiation*, Kluwer Academic Publishers, 497-502 (1999).
- 54 Agosteo, S., Silari, M. and Ulrici, L. *Improved response of bubble detectors to high energy neutrons*. *Radiat. Prot. Dosim.* **88**, 149-155 (2000).
- 55 O'Sullivan, D., Zhou, D., Heinrich, W., Roesler, S., Donnelly, J., Keegan, R., Flood, E. and Tommasino, L. *Cosmic rays and dosimetry at aviation altitudes*. *Radiation Measurements* **31**, 579-584 (1999).
- 56 Spurny, F. *Individual dosimetry for high-energy radiation fields*. *Radiat. Prot. Dosim.* **85**, 15-20 (1999).
- 57 Spurny, F., Trousil, J. and Studena, J. *Response of Czech routine personal dosimeters in high energy radiation reference fields*. *Radiat. Prot. Dosim.* **71**, 181-185 (1997).
- 58 Stewart, R.D., McDonald, J.C., Otto, T. and Loesch, R.M. *Fourth intercomparison of personal dosimeters used in the Department of Energy accelerator facilities*. *Radiat. Prot. Dosim.* **87**, 77-86 (2000).
- 59 Sasaki, M., Nakamura, T., Tsujimura, N., Ueda, O. and Suzuki, T. *Development and characterisation of a real-time personal neutron dosimeter with two silicon detectors*. *Nucl. Instrum. and Meth. A* **418**, 465-475 (1998).
- 60 Heinrich, W., Roesler, S. and Schraube, H. *Physics of cosmic radiation fields*. *Radiat. Prot. Dosim.* **86**, 253-258 (1999).
- 61 McCall, M.J., Green, A.R., Lewis, B.J., Bennet, L.G.I., Pierre, M., Schrewe, U., O'Brien, K. and Feldsberger, E. *Canadian-based aircrew exposure from cosmic radiation on commercial airline routes*. Proceedings of Conference – 21<sup>st</sup> Annual Conference of the Canadian Nuclear Society, Toronto, Ontario, Canada, June 11-14, 2000, ISBN 0-919784-66-6 (2000).
- 62 Curzio, G., Grillmaier, R.E., O'Sullivan, D., Pelliccioni, M., Piermattei, S. and Tommasino, L. *Italian national survey of aircrew exposure: I. Characterisation of advanced instrumentation*. *Radiat. Prot. Dosim.* **93**, 115-123 (2001).
- 63 Badhwar, G.D., Robbins, D.E., Gibbons, F. and Braby, L.A. *Response of a Tissue Equivalent Proportional Counter to neutrons*. Submitted for publication in *Radiation Measurements*.
- 64 Beaujean, R., Kopp, J. and Reitz, G. *Active dosimetry on recent space flights*. *Radiat. Prot. Dosim.* **85**, 223-226 (1999).

- 65 Luszik-Bhadra, M., Matzke, M., Otto, T., Reitz, G. and Schuhmacher, H. *Personal neutron dosimetry in the space station MIR and the space shuttle*. Radiation Measurements **31** 425-430 (1999).
- 66 Luszik-Bhadra, M., Matzke, M. and Schuhmacher, H. *Development of personal neutron doseimeters at the PTB and first measurements in the space station MIR*. Radiation Measurements (in press).
- 67 Luszik-Bhadra, M., d'Errico, F., Hecker, O. and Matzke, M. *A wide-range directional neutron spectrometer*. Nucl. Instrum. and Meth. A (in press).
- 68 Bossler, J., Bouyaya, H., Ferioli, G., Jenninger, B., Policella, Ch., Rieubland, J.M. and Rijllart, A. *Preliminary measurements on microcalorimeters foreseen to be used as beam-loss monitors*. CERN LHC Project Note **71** (1996).
- 69 Gschwendtner, E., Fabjan, C.W., Otto, T. and Vincke, H. *Measuring the photon background in the LHC-experimental environment*. Nucl. Instrum. and Meth. A (in press).
- 70 Heinrich, W. and Sorensen, R.H. *Particle upsets in memory arrays (PUMA)*. Contract F61708-97-W0234, Final report (June 1999).
- 71 Heimers, A. *Cytogenetic analysis in human lymphocytes after exposure to simulated cosmic radiation which reflects the inflight radiation environment*. Int. J. of Radiat. Biol. **75**, 691-698 (1999).
- 72 Alevra, A.V., Klein, H. and Schrewe, U.J. *Measurements with the PTB Bonner Sphere Spectrometer in high-energy neutron calibration fields at CERN*. PTB-Bericht N-22 (1994).
- 73 Dinter, H. and Tesch, K. *Neutron spectra behind the shielding of a high energy proton accelerator: measurements and calculations*. Radiat. Prot. Dosim. **63**, 175-180 (1996).
- 74 Spurny, F. *Dosimetry of neutrons and high energy particles with nuclear track detectors*. Radiation Measurements **25**, 429-436 (1995).
- 75 Bottolier-Depois, J.F., Plawinski, L., Spurny, F. and Mazal, A. *Microdosimetric investigations in realistic fields*. Radiat. Prot. Dosim. **70**, 203-206 (1997).
- 76 Lim, T., Bottolier-Depois, J.F., Festag, J.G., Golnik, N., Grillmaier, R.E., Höfert, M. and Lindborg, L. *Tissue-equivalent proportional counters in a high-energy neutron field at CERN*. Proceedings of Conference – International Conference: Neutrons in Research and Industry, Crete (Greece), 9-15 June 1996, Ed. Vourvopoulos, SPIE Vol. 2867, 300-305 (1997).
- 77 Józefowicz, K., Burgkhardt, B., Vilgis, M. and Piesch, E. *Polycarbonate track detectors with a flat energy response for the measurement of high energy neutrons at accelerators and airflight altitudes*. Radiat. Prot. Dosim. **70**, 143-148 (1997).

- 78 Bartlett, D.T., Hager, L.G., Tanner, R.J. and Steele, J.D. *Measurements of the high energy neutron component of cosmic radiation fields in aircraft using etched track dosimeters*. Radiation Measurements (in press).
- 79 Reitz, G. *Radiation environment in the stratosphere*. Radiat. Prot. Dosim. **48**, 5-20 (1993).
- 80 Armstrong, T.W. and Colborn, B.L. *Monte Carlo predictions of secondary neutron spectra inside the International Space Station and comparison with space measurements*. Proceedings of Workshop - Predictions and Measurements of Secondary Neutrons in Space, USRA, Houston, 1998. Edited by Badhwar, G.D. (1998).